Articles in PresS. J Neurophysiol (September 2, 2015). doi:10.1152/jn.00682.2015

Electrical maturation of spinal neurons in the human fetus: comparison of ventral and dorsal horn

MA Tadros[1], R Lim[1], DI Hughes[2], AM Brichta[1] and RJ Callister[1*]

[1] School of Biomedical Sciences & Pharmacy, Faculty of Health and Medicine, Hunter Medical Research Institute, The University of Newcastle, Callaghan, NSW 2308, Australia

[2] Spinal Cord Research Group, Institute of Neuroscience and Psychology, College of Medical, Veterinary and Life Sciences, University of Glasgow, Glasgow G12 8QQ, United Kingdom

Running Title: development of human spinal neurons

Key Words: action potential, excitability, pain, motoneuron

Address for correspondence:
Dr. R.J. Callister
School of Biomedical Sciences & Pharmacy
The University of Newcastle
Callaghan, NSW 2308
Australia
Phone: Int-61-2-4921-7808
Fax: Int-61-2-4921-8712
Email: robert.callister@newcastle.edu.au

Abstract

The spinal cord is critical for modifying and relaying *sensory* information to, and *motor* commands from, higher centres in the central nervous system to initiate and maintain contextually relevant locomotor responses. Our understanding of how spinal sensorimotor circuits are established during in utero development is based largely on studies in rodents. In contrast, there is little functional data on the development of sensory and motor systems in humans. Here, we use patch clamp electrophysiology to examine the development of neuronal excitability in human fetal spinal cords (10-18 weeks gestation; WG). Transverse spinal cord slices (300 μm thick) were prepared and recordings were made from visualized neurons in either the ventral (VH) or dorsal (DH) horn at 32^{o}C. Action potentials (APs) could be elicited in VH neurons throughout the period examined, but only after 16 WG in DH neurons. At this age, VH neurons discharged multiple APs, whereas most DH neurons discharged single APs. In addition, at 16-18 WG VH neurons also displayed larger AP and after-hyperpolarization amplitudes than DH neurons. Between 10 and 18 WG the intrinsic properties of VH neurons changed markedly, with input resistance decreasing and AP and AHP amplitudes increasing. These findings are consistent with the hypothesis that VH motor circuitry matures more rapidly than the DH circuits that are involved in processing tactile and nociceptive information.

Introduction

The ability to interact appropriately with our environment arises, in part, from the capacity of the spinal cord to receive, modify, and relay sensory information and respond to this information via motor commands that produce coordinated movement. Establishing the underlying circuits requires a complex developmental plan that is first laid-down in the embryo, consolidated in the fetus, and modified throughout life (Fitzgerald 2005; Petersson et al. 2003). Moreover, when this complex developmental plan is interrupted, it can result in adverse consequences for sensorimotor processing in the adult (Baccei 2010; Walker et al. 2009; Zouikr et al. 2014). Our understanding of the important developmental changes that occur in the early stages of spinal cord development come largely from studies in rodents. Collectively, these studies have demonstrated that primary afferents enter the spinal cord to make a myriad of connections with spinal neurons and then undergo substantial fine-tuning to generate a spatio-temporal map of the body within the spinal cord (Granmo et al. 2008; Petersson et al. 2004). Importantly, the intrinsic properties of these spinal neurons are also maturing during the late embryonic and early postnatal stages of development (Baccei 2014; Vinay et al. 2000b; Walsh et al. 2009). Few studies have investigated the functional development of neurons in spinal sensorimotor pathways in humans.

In rodents, specific neuronal subtypes can be identified in the spinal cord by their molecular signatures from ~E10 (Guerout et al. 2014), and electrical activity can be observed soon after. Electrical activity is thought to exist in the embryonic spinal cords of mice at E12, based on recordings of spontaneous rhythmic activity in the sciatic nerve (Hanson and Landmesser 2003). Similarly, in the rat ventral horn (VH) presumptive motoneurons exhibit glycinergic postsynaptic currents from as early as E12.5 (Scain et al. 2010), and discharge antidromic action potentials (APs) by E18 (Di Pasquale et al. 1996). This occurs later in the dorsal horn (DH), where small and very broad APs have been recorded in neurons from E15 mice (Walsh et al. 2009). Taken together, these data suggest that functional development of spinal neurons in rodents occurs in the latter half of *in utero* development.

The capacity of human fetal spinal neurons to generate electrical activity has been examined using cultured spinal cords from 8-10 week-gestation (WG) fetuses.

Electrophysiological studies have shown membrane depolarization in spinal neurons after glutamate application, as well as the presence of voltage-sensitive sodium, potassium, and calcium currents (Hosli et al. 1976; Hosli et al. 1973). These data are supported by anatomical studies that have confirmed the presence of synaptic specialisations between cultured neurons (Kim et al. 1988). Together, these findings suggest at least some of the fundamental elements for neurotransmission and AP generation are present in 8-10 WG fetal spinal neurons. However, the difficulties in establishing viable human neuronal cultures means data are only available over a very restricted time window during the first trimester of human development (Kato et al. 1985; Kennedy et al. 1980).

To address this deficit, we developed a new approach to studying electrophysiological properties of human fetal spinal neurons using acute spinal cord slices prepared from fetuses aged 10 – 18 WG. We used this preparation to investigate how the electrophysiological properties of neurons in the ventral and dorsal horns of the grey matter mature over 8 weeks of fetal development. Such investigations are important for translation of findings made in rodents to humans (see (Davidson et al. 2014).

Methods

Tissue preparation

All procedures were approved by the University of Newcastle Human Research Ethics Committee (HREC). Written consent was obtained from all tissue donors prior to termination and all associated information remained at the clinic. Products of conception (POC) were only obtained from elective terminations, and there were no known abnormalities in our samples. Apart from gestational age (which ranged from 10 to 18 weeks), no identifying information was supplied to researchers. Gestational age was determined using three criteria: 1) date of the last menstrual period; 2) ultrasound measurements of crown-rump length (CRL); and 3) foot length (Hern 1984). POCs were collected in cold glycerol-substituted artificial cerebrospinal fluid (gACSF) containing (in mM): 250 glycerol, 26 $NaHCO_3$, 11 glucose, 2.5 KCl, 1.2 NaH_2PO_4, 1.2 $MgCl_2$ and 2.5 $CaCl_2$ bubbled with 95% O_2 and 5% CO_2 (Ye et al. 2006). gACSF was used in place of the traditional sucrose-substituted ACSF (Walsh et al. 2009) as it improved slice viability, and importantly, allowed sharing of valuable tissue across multiple projects, including placental studies (Pringle et al. 2011) and investigation of vestibular hair cell development (Lim et al. 2014). All samples were delivered to the laboratory within 1 hour of the termination procedure. Vertebral columns were isolated and transferred to a dissecting chamber containing ice-cold gACSF continuously bubbled with 95% O_2 and 5% CO_2. The spinal cord was removed and transverse slices of the lumbosacral region (300 μm thick) were obtained using a vibrating-blade microtome (Leica VT1200S; Leica Microsystems, Wetzlar, Germany). Spinal cord slices were then transferred to a humidified storage chamber containing oxygenated ACSF (118 mM NaCl substituted for glycerol in the gACSF). Slices were allowed to incubate for 1 h at room temperature (22 - 24^{o}C) before recording commenced.

Electrophysiology

Spinal cord slices were transferred to a recording chamber and held in place using nylon netting fixed to a U-shaped platinum frame (Fig 1A). The recording chamber was continually superfused with oxygenated ACSF (4-6 bath volumes/minute) and maintained at near-physiological temperature (32^{o}C) using an in-line temperature

control device (TC-324B; Warner Instruments, Hamden, CT). Whole cell patch clamp recordings were obtained from spinal neurons in either ventral or dorsal horn (VH or DH cells, respectively), visualised using infrared differential contrast optics (IR-DIC optics, Fig 1B) and an IR-sensitive camera (Rolera-XR; QImaging, Surrey, Canada). For VH cells, we deliberately targeted the largest neurons as these are considered presumptive motoneurons (Carlin et al. 2000). At the end of each recording session, the location of the recorded neuron was documented using still images of the spinal cord while the patch pipette remained in place (Fig 1C).

Patch pipettes (3 to 5 MΩ resistance) were pulled from thin-walled borosilicate glass (PG150T-15; Harvard Apparatus, Kent, UK) and filled with a potassium-based internal solution containing the following (in mM): 135 KCH_3SO_4, 6 NaCl, 2 $MgCl_2$, 10 HEPES, 0.1 EGTA, 2 MgATP and 0.3 NaGTP (pH 7.3, using KOH). Whole cell patch clamp recordings were made using a Multiclamp 700B Amplifier (Molecular Devices, Sunnyvale, CA). The whole cell recording configuration was first established on visualized neurons in voltage-clamp (holding potential -60 mV). Series resistance and input resistance (R_{IN}) were measured from the averaged response (5 trials) to a 5 mV hyperpolarizing pulse. These parameters were measured at the beginning, and end of each recording session and data were rejected if values changed by > 20%. After determining series and input resistances, the recording mode was switched to current clamp and the membrane potential observed after ~ 15 s was designated as resting membrane potential (RMP). All subsequent current clamp recordings were made from this potential. The capacity of neurons to discharge action potentials (APs) was assessed by injecting a series of depolarizing current steps (Tadros et al. 2014; Tadros et al. 2012). Due to generally lower input resistance in VH neurons, we used 50 pA increments, 1 second duration while for higher resistance DH neurons we used 20 pA increments, 800 ms duration. Similarly, the potential for rebound discharge was assessed by hyperpolarizing current steps, -50 pA increments, 1 second duration for VH neurons, and -20 pA increments, 800 ms for DH neurons.

Data capture and analysis

Data were digitised on-line (sampled at 20 kHz, filtered at 6 kHz) via an ITC-16 computer interface (Instrutech, Long Island, NY) and captured on a Macintosh

computer using Axograph X software (Axograph X, Sydney, Australia). All data were analysed offline using the Axograph software. RMP and AP threshold were corrected for a calculated liquid junction potential of ~ 10 mV (Barry and Lynch 1991). Individual APs were detected using the derivative threshold method (range of 15-20 mV/ms, Graham et al. 2007b). AP threshold was measured at the inflection point during the rising phase of the AP (ie, when dV/dt exceeded 15-20 mV/ms). Rheobase current was defined as the minimum step-current that could evoke at least one AP. The amplitude of each AP was measured between threshold and maximum positive peak and AHP amplitude was measured as the difference between AP threshold and the maximum negative peak. AP half width was calculated at 50% of the maximum positive peak and AHP half width was measured at 50% of the maximum negative peak. AHP half width was chosen as a measure of AHP duration as it was often hard to determine precisely when membrane potential returned to rest, especially in tonic firing neurons.

SPSS v21 software package (SPSS, Chicago, IL) was used for statistical analysis. Student's T-tests were used to compare VH and DH data when such comparisons could be made, and one-way ANOVA was used to compare means across age groups. Scheffe's post hoc tests were used to determine where means differed. Data sets that failed Levene's test of homogeneity of variance were compared using non-parametric Mann-Whitney or Kruskal-Wallace tests, followed by Tamhame's T2 post hoc test. G-tests, with Williams's correction, were used to determine whether the prevalence of AP discharge categories, responses to hyperpolarizing steps and spontaneous activity differed between ages and regions of the spinal cord. Statistical significance was set at $p < 0.05$ and all data are presented as means ± SEM.

Results

Recordings were obtained from 91 neurons in 17 fetuses aged 10-18 WG. To compare the properties of neurons with the best available behavioural (reflex/movement) data, we assigned recorded neurons into one of three age groups: 10-12 WG, 13-15 WG, and 16-18 WG. These groups were selected as they represent times when mouth opening reflexes elicited by cutaneous stimulation (touching or stroking) with "…a hair tipped with smooth inert material…" fall into three phases (Humphrey 1969). Reflexes first appear at 10-12 WG, become more complex at 13-14 WG, before appearing less stereotyped and "more graceful and flowing" after 16 WG (Humphrey 1969). Recordings were made from visualized neurons in either the ventral (VH) or dorsal horn (DH) and the location of recorded neurons in representative transverse spinal cord sections for each of the three age groups is shown in Figure 1.

We were able to obtain recordings from VH neurons in all three age groups as they were easily identified and more securely embedded in the spinal cord (Fig 1B). In contrast, obtaining patch clamp recordings from DH neurons in spinal cords younger than 16 WG proved to be technically challenging: few recordings were obtained in the 10-12 WG and 13-15 WG groups (Fig 1C, left and middle panels, n = 2 and 1, respectively). Before 16 WG, DH neurons were extremely small, appeared to lack dendrites, and were weakly tethered in the spinal cord neuropil (Fig 1B). This meant the positive pressure required for successful patch clamp recordings pushed neurons away from the recording electrode, and often ejected them out of the spinal cord slice. Importantly, optimal recordings of VH neurons were obtained in the same slices where these features were observed in DH neurons. Furthermore, none of the small neurons, which dominated in the DH, were observed in the VH at any age. This suggests slice quality was not an issue in achieving adequate patch clamp recordings of DH neurons prior to 16 WG.

Spinal neurons' capacity to discharge action potentials

The capacity of neurons to discharge APs was assessed by injecting a series of depolarizing current steps of increasing amplitude. One of four types/patterns of AP discharge was observed in each recorded neuron (Fig 2A). *Tonic firing* neurons discharged APs for the entire duration of the current injection, and increased their

discharge frequency with increasing current amplitude. *Initial bursting* neurons were characterised by a brief, high frequency burst of APs at the onset of the current step. *Single spiking* neurons discharged a single AP immediately upon depolarization, regardless of current intensity. *Reluctant firing* neurons did not discharge APs in response to current injection, despite depolarization well above mean AP threshold (see Fig 2A, bottom right panel). These neurons were included in our analysis as their intrinsic properties fell within the range observed in those that discharged APs in response to current injection in their respective age groups. We have also observed reluctant firing neurons in previous studies of spinal neurons in postnatal rodent models, both in vitro and in vivo (Graham et al. 2004; Walsh et al. 2009).

There were notable differences in the capacity of VH and DH neurons to generate APs following depolarizing current injection (Fig 2B & C). For VH neurons, the four discharge categories were observed at all ages (Fig 2C). Tonic firing was the most commonly observed discharge pattern and its incidence increased significantly with age (12/22, 55% at 10-12 WG and 15/23, 65% at 16-18 WG, $p = 0.025$). This was accompanied by a significant decrease in the prevalence of reluctant firing neurons (7/22, 32% at 10-12 WG vs. 1/23, 4% at 16-18 WG, $p = 0.014$). The proportion of initial bursting and single spiking neurons was similar across the three age groups (initial bursting: 1/22, 5% at 10-12 WG vs. 2/23, 9% at 16-18 WG, $p = 0.57$; single spiking: 2/22, 9% at 10-12 WG vs. 5/23, 22% at 16-18 WG, $p = 0.21$; see Fig 2C).

In slices younger than 16 WG we did not record APs in DH neurons mainly due to the difficulties encountered in establishing reliable seals on neurons in these two younger age groups (described above). From 16 WG, however, over half the DH neurons discharged APs and exhibited either tonic firing (3/15, 20%) or single spiking (6/15, 40%, Fig 2B) profiles. A comparison of the various AP discharge patterns in VH and DH at 16-18 WG revealed a significant difference in the proportions of these patterns ($p = 0.003$, Fig 2B & C), with VH neurons displaying less single spiking or reluctant firing neurons compared to the DH sample. We never observed delayed firing neurons in the DH, which have been considered to be excitatory interneurons in the mature rodent DH (Lu et al. 2006). Together, these data suggest the adult proportions of excitatory and inhibitory DH neurons is yet to be established because the mature rodent DH exhibits all major discharge patterns (Lu et al. 2006; Walsh et al. 2009).

We next compared the intrinsic and AP properties across the discharge categories for each age group. Although statistics were limited in some instances, we noted several significant differences between certain populations (Table 1). At all three age groups, tonic firing neurons in the VH displayed more hyperpolarized RMPs compared to the other discharge categories, with greater AP and AHP amplitudes than single spiking neurons at both 13-15 WG and 16-18 WG, as well as initial bursters at 16-18 WG. These differences between tonic firing and single spiking neurons have been observed in rodent DH neurons during development (Walsh et al. 2009; Tadros et al. 2012), suggesting the characteristics of each discharge category are consistent across species.

Responses to hyperpolarizing current

We have shown previously that developing spinal and brainstem neurons in rodents respond to hyperpolarizing current in one of four ways (Tadros et al. 2014; Tadros et al. 2012). Similar types of responses were observed in human fetal VH and DH neurons (Fig 3A). *Passive* responses were characterized by the absence of active conductances during or after the hyperpolarization step. *Rebound spiking* responses featured AP discharge upon release from hyperpolarization. Such responses have been associated with the low threshold T-type calcium current in adult rodent spinal neurons (Graham et al. 2007b; Yoshimura and Jessell 1989). In some neurons we observed a "sag" in the voltage trace during the hyperpolarization step, which is typically associated with the hyperpolarization-activated mixed cationic inward current (I_h; Graham et al. 2007b; Yoshimura and Jessell 1989). Finally, some neurons exhibit a "sag" indicative of I_h as well as an extended hyperpolarization following release from current injection. This extended hyperpolarization is known to be dependent on extracellular potassium concentration (Yoshimura and Jessell 1989), and could be driven by either a calcium activated potassium conductance, or A-type potassium currents (Callister et al. 1997; Graham et al. 2007b).

Responses to hyperpolarizing current injection displayed greater variability in VH neurons than in DH (Fig 3C) and could be compared across the three age groups. Rebound spiking was observed in 17/22 (77%; 10-12 WG) and 10/23 (44%; 13-15 WG) VH neurons. In the 16-18 WG age group all four responses were observed with 6/23 (26%) neurons showing a passive response, 12/23 (52%) displaying rebound

spiking, 4/23 (18%) exhibiting the voltage-sag characteristic of I_h current and only 1/23 (4%) neurons showing both the "sag" and extended hyperpolarization. Prior to 16 WG, DH neurons exhibited passive responses during hyperpolarizing current injection (n=3). Such responses also dominated in the 16-18 WG group (9/15; 60%), however rebound spiking (3/15; 20%) and the extended hyperpolarizing response (3/15; 20%) were also observed (Fig 3B). Interestingly, the proportions of each response to hyperpolarizing current differed significantly between the VH and DH neurons at 16-18 WG (p=0.01, Fig 3B & C). These data further emphasise the differences between VH and DH at 16-18 WG and suggest the responses to hyperpolarizing current injection become more variable with age in VH neurons.

Differences between VH and DH neurons

We next compared the intrinsic and AP properties of VH and DH neurons that were capable of AP discharge at 16-18 WG (Fig 4A). VH neurons had lower input resistances (mean = 341 vs. 664 MΩ, p = 0.05), and higher rheobase currents (141 vs. 64 pA, p = 0.29) than DH neurons. RMP was similar (~ -75 mV) in VH and DH neurons (Fig 4A). It is notable that including all neurons (those that did and did not discharge APs) in the above analysis increased variability and minimised statistical differences, because both intrinsic and AP properties differed across the various discharge categories observed in spinal neurons (Graham et al. 2007a; Tadros et al. 2012).

AP discharge was not observed in the limited recordings made in 10-12 WG and 13-15 WG DH neurons. There was also a significant difference in the proportion of various AP discharge patterns (p = 0.003, Fig 2B & C) and responses to hyperpolarizing current (p = 0.01, Fig 3B & C) in VH and DH neurons at 16-18 WG (p = 0.003, Fig 2B & C). Spontaneous AP discharge was observed in some neurons (Fig 4B). In VH, spontaneous activity was observed in all three age groups. Predictably, spontaneous activity was not observed in DH until 16-18 WG, when 3/15 (20%) neurons displayed spontaneous AP discharge. The prevalence of spontaneous AP discharge at 16-18 WG in DH was similar to that observed in VH (7/23, 30%, p = 0.6). These data provide further evidence that VH neurons develop more rapidly than DH neurons in the human fetal spinal cord.

AP properties were measured on rheobase APs, that is, the first AP elicited in response to depolarizing current injection (Fig 4C). AP threshold was similar in VH and DH neurons (~ - 53 mV), although AP amplitude (VH; 47.3 ± 3.4 mV vs. DH; 29.7 ± 6.7, p = 0.015) and AHP amplitude (VH; -18.8 ± 2.0 vs. DH; -6.5 ± 1.5 mV, p = 0.001) were greater in VH neurons. AP half width was not different between VH and DH neurons (2.1 ± 0.4 vs. 2.7 ± 0.3 ms, p = 0.32). Even though AP half width did not differ, we found a significantly greater dV/dt on the rising phase of the AP in VH neurons (126.0 ± 16.2 vs. 38.9 ± 16.0 V/s, p = 0.005), suggesting the underlying depolarizing currents contributing to the AP differ between VH and DH neurons. We also found a greater AHP half width (ie, duration at 50% of the maximum negative peak) in VH neurons (VH; 83.1 ± 15.7 ms vs. DH; 25.9 ± 11.0 ms, p = 0.02). This is consistent with the larger AHP amplitude in VH neurons. Taken together, these differences in intrinsic and AP properties imply larger, faster, APs in VH neurons, which is clearly illustrated by the example APs shown in the right panel of Figure 4C.

Development of intrinsic and AP properties in VH neurons

Intrinsic and AP properties of VH neurons were also compared across the three age groups. Spontaneous AP discharge was observed at all three ages and its prevalence did not change significantly with age (8/22 (36%) at 10-12 WG; 6/26 (23%) at 13-15 WG; and 7/23 (30%) at 16-18 WG; p = 0.6, Fig 4B). Comparisons of intrinsic and AP properties in VH neurons were restricted to neurons that exhibited the tonic discharge pattern for two reasons. First, intrinsic and AP properties differ in spinal neurons according to AP discharge type (Tadros et al. 2012; Walsh et al. 2009). Second, tonic firing neurons were the dominant AP discharge category at all three ages examined (n = 12 (55%) for 10-12 WG; n = 12 (50%) for 13-15 WG; n = 15 (65%) for 16-18 WG).

Several intrinsic properties of tonically firing VH neurons changed during the developmental period examined (Fig 5). Input resistance (R_{IN}) decreased from 795 ± 145 MΩ at 10-12 WG to 238 ± 83 MΩ at 16-18 WG (p = 0.004) and rheobase current increased from 50 pA at 10-12 WG to 117 ± 30 pA at 16-18 WG (p = 0.04). The difference in rheobase current is likely to be an underestimate since the smallest current step we used (i.e., 50 pA) elicited APs in all VH neurons at 10-12 WG. RMP

and AP threshold were unchanged at ~ -70 mV and ~ - 45 mV, respectively (Fig 5A, RMP; Fig 5B, AP threshold) between the three age groups. Several AP properties changed dramatically between 10-12 WG and 16-18 WG. Specifically, AP amplitude increased (10-12 WG; 44.8 ± 3.6 mV vs. 16-18 WG; 56.5 ± 1.8 mV, $p = 0.01$) and AP half width decreased (10-12 WG; 3.03 ± 0.61 ms vs. 16-18 WG; 1.30 ± 0.21 ms, $p = 0.001$). AHP amplitude also increased over this developmental period (10-12 WG; -9.2 ± 2.4 mV vs. 16-18 WG; -23.3 ± 1.7 mV, $p = 0.001$; Fig 5B), and was accompanied by an increase in the AHP half width (10-12 WG; 39.7 ± 13.5 ms vs. 16-18 WG; 107.0 ± 19.5 ms, $p = 0.016$). Together, these data suggest the intrinsic and AP properties of tonic firing VH neurons undergo significant maturation between 10 and 18 WG in the human fetus.

Discussion

Here, we provide functional data on the intrinsic properties of VH and DH neurons in acute slices prepared from first and early second trimester human fetal spinal cords. We document dramatic changes in the intrinsic and action potential properties of VH spinal neurons during this developmental period. In contrast, we were unable to record APs from DH neurons prior to 16 WG, which may indicate differences in the development of electrical activity in the dorsal and ventral horns of the human fetal spinal cord. These findings are consistent with classical anatomical (Okado et al., 1979; Okado 1981; Sarnat et al. 1998; Ray and Wadhwa 1999) and clinical studies (de Vries et al. 1985; Slater et al. 2010b) that indicate functional connectivity develops earlier within motor circuits compared to those in the DH involved in processing tactile and nociceptive information.

Previous studies investigating electrical properties of human fetal spinal neurons

To our knowledge, the functional properties of human spinal neurons have only been examined in cultured fetal neurons. Early functional studies, using sharp microelectrode recording in long-term cultures (22 days) prepared from a 17 WG fetus, reported input resistances of ~ 5 MΩ (3 neurons) and RMPs of ~ - 44 mV (25 neurons; Hosli et al. 1973). These values are much lower than those we recorded at any gestational age (Fig 4A and 5A). Notably, the authors stated "the membrane potential of most cells decayed within 20-40 sec after impalement". In that study the response of neurons to depolarizing or hyperpolarizing current injection could not be examined. Later work by the same group recorded dose-dependent depolarizations to bath-applied excitatory amino acids (glutamate and aspartate) in neurons cultured (8-56 days) from 7-17 WG fetuses (Hosli et al. 1976). These important data show human spinal neurons in culture express ligand gated ion channels for major excitatory neurotransmitters. However, the neurons sampled in the above study came from fetuses of varying ages and different times in culture. This makes it difficult to establish precisely the spatiotemporal expression of receptor channels and their subunits *in situ.* In future studies it will be possible to use the recording techniques used in our study, combined with sophisticated electrophysiological methodologies, to

answer these important questions using *in situ* spinal neurons in VH and DH populations.

Subsequent studies using patch clamp recordings from spinal neurons, grown in long-term cultures (19-20 days) from 8-9 WG fetuses report RMPs of ~ - 40 mV (Kato et al. 1985). Here at later stages of development, we report substantially more hyperpolarized RMP (~ -75 mV). In contrast, we have shown similar AP half width (~ 2 ms; Fig 4C) to previous findings where short duration APs were recorded in cultured neurons in response to current injection. In those cultured neurons, TTX-sensitive sodium, TEA and 4-AP sensitive potassium, and cobalt-sensitive calcium currents are also present (Kato et al., 1985).

It is difficult to determine in the above study whether the cultured neurons were dorsal or ventral horn in origin, although attempts were made to identify motoneurons using acetylcholinesterase immunohistochemistry (Kato et al., 1985). APs have been examined in VH neurons grown in long term cultures (9 weeks) from 8 WG fetuses, however, these VH neurons only discharged single and slow APs in response to depolarizing current injection (Kim et al. 1988). These results are in contrast to ours that show VH neurons have robust, repetitive AP discharge from 10 WG (Fig 4). It is therefore likely that neurons recorded in spinal cord slices from fetuses aged 10-18 WG are more representative of neurons *in situ* than those in culture, as they display more diverse electrical properties.

Comparison of the electrical properties of rodent and fetal spinal neurons

Ventral horn neurons

The most comprehensive data investigating the development of intrinsic properties in VH neurons prior to birth comes from rodent studies. In rats, sodium, calcium, and potassium conductances can be recorded in VH neurons at E14, and large overshooting sodium-dependent APs are generated a few days later (Ziskind-Conhaim 1988). In respiratory motoneurons, electrical properties including RMP, input resistance, and rheobase current have been shown to change during the course of development (Di Pasquale et al. 1996). Here, we show similar developmental changes in human fetal VH neurons, with dramatic changes in both intrinsic and AP properties

occurring between 10 and 18 WG (Fig 4). We cannot conclusively determine whether our VH neurons were motoneurons. In early experiments we attempted to fill recorded neurons and then stain for choline acetyltransferase (ChAT) to determine their identity. This could not be achieved, as our spinal cord slices did not survive fixation and subsequent processing. We assume this is due to the lack of connective tissue in the developing nervous system (Weidenheim et al. 1993). However, we deliberately targeted large neurons in the VH and so it would be reasonable to assume these were nascent motoneurons. Tonic (or repetitive) firing has long been considered a distinguishing feature of adult spinal motoneurons (Brownstone 2006), however, early postnatal spinal MNs can generate bursting and even single spiking AP discharge patterns in rats (Vinay et al. 2000a). In our sample of fetal human VH neurons, we observed each of these three discharge patterns (Fig 2B), suggesting that the electrophysiological profile observed in the human fetus is similar to rodent VH neurons during postnatal development. It appears that the greatest difference between human and rodent VH neurons is when these discharge patterns are expressed.

Dorsal horn neurons

Our recent study examined the intrinsic properties of neurons in DH outer laminae in mice during late embryonic (E15-17) development (Walsh et al. 2009). After birth, AP properties continue to mature, with increases in AP and AHP amplitudes and decreases in AP half width, until they exhibit adult-like characteristics at ~P10. AP discharge patterns also changed from predominately single spiking at E15-17 to bursting and tonic firing discharge patterns at P10 (Walsh et al. 2009). Although we could only measure AP properties and discharge at one time-point (16-18 WG) for human DH neurons (Fig 4), it appears they mature much earlier than their rodent counterparts (i.e., in the first vs. latter half of gestation). The predominant discharge patterns observed in human fetal DH neurons were single spiking and reluctant firing (Fig 2C), similar to that observed in embryonic mice (Walsh et al. 2009).

Functional connectivity within the developing sensorimotor system

During development, axons of VH neurons exit the spinal cord and ultimately innervate skeletal muscle (Vermeren et al. 2003). The timing of this process has been studied extensively in rodents. For example, the phrenic nerve enters the diaphragm as early as E15 and neuromuscular junctions are formed by E18-19 (Bennett and

Pettigrew 1974). Based on the presence of end plate potentials recorded in the diaphragm, these junctions are functional by E17-22 (Diamond and Miledi 1962). As the rat gestation period is 21-23 days, functional connections between nerve and muscle occur very late during intrauterine development in this species. In contrast, motor end plates are present very early in human development - in quadriceps at 9 WG (Fidzianska 1980), intercostal muscles at 8.5 WG, tibialis anterior at 10 WG (Juntunen and Teravainen 1972) and masseter at 12 WG (Ezure 1996). To our knowledge, endplate potentials have not been recorded from developing human neuromuscular junctions. However, studies conducted over half a century ago considered the emergence of movement and spinal reflexes in the human fetus as evidence of functional connectivity between nerve and muscle. Specifically, reflex responses to cutaneous stimulation of the perioral region can be observed as early as 7.5 WG and movement complexity to the same stimuli increases over the next 10 weeks (summarised in Humphrey 1969). Furthermore, histological studies on fibre projections and spinal cord cytology in early stage human fetuses, coupled to clinical observations, have proposed that spinal reflex mechanisms are established by 8 WG (Windle and Fitzgerald, 1937; Hooker, 1936). Ultrasound imaging has also shown that the human fetus is capable of reflex movement very early in development (de Vries et al. 1985). Our data showing VH neurons discharge trains of APs from 10 WG (Fig 2C), coupled with the presence of neuromuscular junctions is consistent with the existence of well-established connections between VH neurons and skeletal muscle in the first trimester of pregnancy.

In contrast to VH neurons, our study suggests DH neurons are very immature and incapable of discharging APs prior to 16 WG (Fig 2B). As a consequence, it is unlikely DH neurons are capable of processing sensory inputs before 16 WG. The lack of APs in our study does not necessarily confirm that DH neurons are unexcitable prior to 16WG. However, our findings are consistent with previous anatomical studies on human fetal spinal cords that demonstrate a lack of NeuN staining in the DH despite strong staining in the VH at 10 WG (Sarnat et al. 1998). Similarly, very low Nissl staining has been observed in the DH at 12-13 WG (Ray and Wadhwa 1999). In addition, a “sparse” number of sensory axons terminals have been observed in DH superficial lamina as late as 19 WG (Konstantinidou et al. 1995). However, the authors were unable to confirm whether the lack of terminals in the DH arose from

technical considerations associated with DiI transport in small axons or true developmental mechanisms. Nevertheless, the lack of responsiveness of DH neurons in our study (Fig 2) indicates that the components of DH sensory pathways are not fully mature prior to 16 WG in the human. Further evidence suggests that DH circuits develop later than those in the VH come from electron microscopic studies of the human fetal spinal cord (Okado 1981; Okado et al. 1979). These studies show that synaptic junctions in the human spinal cord are visible at 5 WG, and are present in the motor neuropil of the VH well before other spinal regions.

Spinal reflexes and pain responses in the human fetus

Meaningful movement depends, in part, on how sensory feedback from receptors located in muscles, joints and skin is processed in spinal circuits. Anatomical studies in rodents demonstrate sensory afferent fibre entry to the spinal cord is dependent upon afferent axon diameter. The largest peripheral afferents enter the spinal cord at ~E15 in rats and reach the VH by E16 (Snider et al. 1992). Functional studies have shown that monosynaptic connections are established with presumed motoneurons in VH by E18 (Kudo and Yamada 1987). By E17, other large diameter fibres occupy the entire DH (Snider et al. 1992) and deep DH neurons respond to stimulation of skin afferents from E18 (Fitzgerald 1991). In contrast small diameter Aδ and C-fibre nociceptive afferents enter the DH later, at ~ E17, and neurons in the superficial DH only appear to connect with these peripheral afferents close to birth (Fitzgerald 2005). Together these data suggest that classical spinal pain circuits involving small diameter fibres that terminate in the superficial DH in rodents are poorly developed, if at all, before birth (Fitzgerald and Jennings 1999; Woodbury and Koerber 2003).

Our data show that DH neurons are capable of discharging APs after 16 WG suggesting that ascending pain pathways are incomplete in the human fetus prior to 16 WG. Importantly, the “pain experience” requires a functional ascending pain pathway, whereby peripherally generated noxious signals reach the spinal cord, and are then relayed to the somatosensory cortex. Electrophysiological studies on newborn humans have demonstrated cortical potentials in response to noxious procedures that break the skin (Slater et al. 2010b). These data suggest most components of the pain neuroaxis are fully formed at birth. Importantly, repeated

552 noxious stimulation of the skin can lead to persistent changes in this pathway and
553 result in exaggerated cortical responses to acute noxious stimulation (Slater et al.
554 2010a). One important question arising from these observations is when does the
555 ascending pain pathway assemble in utero? Recent work using cerebral oxygen
556 changes, as a measure of cortical activity, has shown that acute noxious stimuli (heel
557 lances for routine blood sampling) is transmitted to the somatosensory cortex in the
558 fetus as young as 25 WG (Slater et al. 2006). Taken together, our study and the
559 available data on cortical processing in the developing human suggest the ascending
560 pain pathway is assembled between 16 WG and 25 WG.
561
562 ***Major conclusions and future directions***
563 This study presents the first data acquired from VH and DH neurons in acute spinal
564 cord slices from the human fetus. We have shown that patch clamp recordings can be
565 made from *in situ* VH neurons from 10 WG and that at this age they can discharge
566 APs in response to depolarizing current. In contrast, recordings from DH neurons
567 before 16 WG proved to be difficult - we could not record APs in DH neurons until
568 16 WG. Comparisons made between the intrinsic properties of VH and DH neurons at
569 16-18 WG suggest VH neurons, and VH circuitry, develop weeks before their
570 counterparts in DH. This conclusion is consistent with available anatomical data for
571 the human fetus, which shows peripheral afferents reach the VH and arborize well
572 before they do so in the DH. Our data also have important implications for estimating
573 when the human fetus can experience pain. Neurons in the DH are the first central
574 target for peripheral afferents that carry nociceptive and tactile information. As these
575 neurons are electrically/functionally immature prior to 16 WG it is unlikely that
576 nociceptive information could be processed in the DH and subsequently passed onto
577 supraspinal sites within the pain neuroaxis at this time during development.
578

579 ***References***

580 **Baccei ML**. Modulation of developing dorsal horn synapses by tissue injury. *Annals*
581 *of the New York Academy of Sciences* 1198: 159-167, 2010.
582 **Baccei ML**. Pacemaker Neurons and the Development of Nociception. *Neuroscientist*
583 20: 197-202, 2014.
584 **Barry PH, and Lynch JW**. Liquid junction potentials and small cell effects in patch-
585 clamp analysis. *J Membr Biol* 121: 101-117, 1991.
586 **Bennett MR, and Pettigrew AG**. The formation of synapses in striated muscle
587 during development. *J Physiol* 241: 515-545, 1974.
588 **Brownstone RM**. Beginning at the end: repetitive firing properties in the final
589 common pathway. *Prog Neurobiol* 78: 156-172, 2006.
590 **Callister RJ, Keast JR, and Sah P**. Ca(2+)-activated K+ channels in rat otic
591 ganglion cells: role of Ca2+ entry via Ca2+ channels and nicotinic receptors. *J*
592 *Physiol* 500 (Pt 3): 571-582, 1997.
593 **Carlin KP, Jiang Z, and Brownstone RM**. Characterization of calcium currents in
594 functionally mature mouse spinal motoneurons. *Eur J Neurosci* 12: 1624-1634, 2000.
595 **Davidson S, Copits BA, Zhang J, Page G, Ghetti A, and Gereau RWt**. Human
596 sensory neurons: Membrane properties and sensitization by inflammatory mediators.
597 *Pain* 155: 1861-1870, 2014.
598 **de Vries JI, Visser GH, and Prechtl HF**. The emergence of fetal behaviour. II.
599 Quantitative aspects. *Early Hum Dev* 12: 99-120, 1985.
600 **Di Pasquale E, Tell F, Monteau R, and Hilaire G**. Perinatal developmental changes
601 in respiratory activity of medullary and spinal neurons: an in vitro study on fetal and
602 newborn rats. *Brain Res Dev Brain Res* 91: 121-130, 1996.
603 **Diamond J, and Miledi R**. A study of foetal and new-born rat muscle fibres. *J*
604 *Physiol* 162: 393-408, 1962.
605 **Ezure H**. Development of the motor endplates in the masseter muscle in the human
606 fetus. *Ann Anat* 178: 15-23, 1996.
607 **Fidzianska A**. Human ontogenesis. II. Development of the human neuromuscular
608 junction. *J Neuropathol Exp Neurol* 39: 606-615, 1980.
609 **Fitzgerald M**. The development of nociceptive circuits. *Nat Rev Neurosci* 6: 507-520,
610 2005.
611 **Fitzgerald M**. A physiological study of the prenatal development of cutaneous
612 sensory inputs to dorsal horn cells in the rat. *J Physiol* 432: 473-482, 1991.
613 **Fitzgerald M, and Jennings E**. The postnatal development of spinal sensory
614 processing. *Proc Natl Acad Sci USA* 96: 7719-7722, 1999.
615 **Graham B, Brichta A, and Callister R**. Pinch-current injection defines two
616 discharge profiles in mouse superficial dorsal horn neurones, in vitro. *J Physiol*
617 *(Lond)* 578: 787-798, 2007a.
618 **Graham BA, Brichta AM, and Callister RJ**. In vivo responses of mouse superficial
619 dorsal horn neurones to both current injection and peripheral cutaneous stimulation. *J*
620 *Physiol (Lond)* 561: 749-763, 2004.
621 **Graham BA, Brichta AM, Schofield PR, and Callister RJ**. Altered potassium
622 channel function in the superficial dorsal horn of the spastic mouse. *J Physiol (Lond)*
623 584: 121-136, 2007b.
624 **Granmo M, Petersson P, and Schouenborg J**. Action-based body maps in the spinal
625 cord emerge from a transitory floating organization. *J Neurosci* 28: 5494-5503, 2008.
626 **Guerout N, Li X, and Barnabe-Heider F**. Cell fate control in the developing central
627 nervous system. *Exp Cell Res* 321: 77-83, 2014.

Hanson MG, and Landmesser LT. Characterization of the circuits that generate spontaneous episodes of activity in the early embryonic mouse spinal cord. *J Neurosci* 23: 587-600, 2003.
Hern WM. Correlation of fetal age and measurements between 10 and 26 weeks of gestation. *Obstet Gynecol* 63: 26-32, 1984.
Hosli L, Andres PF, and Hosli E. Ionic mechanisms associated with the depolarization by glutamate and aspartate on human and rat spinal neurones in tissue culture. *Pflugers Arch* 363: 43-48, 1976.
Hosli L, Hosli E, and Andres PF. Light microscopic and electrophysiological studies of cultured human central nervous tissue. *Eur Neurol* 9: 121-130, 1973.
Humphrey T. The relation between human fetal mouth opening reflexes and closure of the palate. *The American journal of anatomy* 125: 317-344, 1969.
Juntunen J, and Teravainen H. Structural development of myoneural junctions in the human embryo. *Histochemie* 32: 107-112, 1972.
Kato AC, Touzeau G, Bertrand D, and Bader CR. Human spinal cord neurons in dissociated monolayer cultures: morphological, biochemical, and electrophysiological properties. *J Neurosci* 5: 2750-2761, 1985.
Kennedy PG, Lisak RP, and Raff MC. Cell type-specific markers for human glial and neuronal cells in culture. *Lab Invest* 43: 342-351, 1980.
Kim SU, Osborne DN, Kim MW, Spigelman I, Puil E, Shin DH, and Eisen A. Long-term culture of human fetal spinal cord neurons: morphological, immunocytochemical and electrophysiological characteristics. *Neuroscience* 25: 659-670, 1988.
Konstantinidou AD, Silos-Santiago I, Flaris N, and Snider WD. Development of the primary afferent projection in human spinal cord. *J Comp Neurol* 354: 11-12, 1995.
Kudo N, and Yamada T. Morphological and physiological studies of development of the monosynaptic reflex pathway in the rat lumbar spinal cord. *J Physiol* 389: 441-459, 1987.
Lim R, Drury HR, Camp AJ, Tadros MA, Callister RJ, and Brichta AM. Preliminary Characterization of Voltage-Activated Whole-Cell Currents in Developing Human Vestibular Hair Cells and Calyx Afferent Terminals. *J Assoc Res Otolaryngol* 2014.
Lu VB, Moran TD, Balasubramanyan S, Alier KA, Dryden WF, Colmers WF, and Smith PA. Substantia Gelatinosa neurons in defined-medium organotypic slice culture are similar to those in acute slices from young adult rats. *Pain* 121: 261-275, 2006.
Okado N. Onset of synapse formation in the human spinal cord. *J Comp Neurol* 201: 211-219, 1981.
Okado N, Kakimi S, and Kojima T. Synaptogenesis in the cervical cord of the human embryo: sequence of synapse formation in a spinal reflex pathway. *J Comp Neurol* 184: 491-518, 1979.
Petersson P, Granmo M, and Schouenborg J. Properties of an adult spinal sensorimotor circuit shaped through early postnatal experience. *J Neurophysiol* 92: 280-288, 2004.
Petersson P, Waldenström A, Fåhraeus C, and Schouenborg J. Spontaneous muscle twitches during sleep guide spinal self-organization. *Nature* 424: 72-75, 2003.
Pringle KG, Tadros MA, Callister RJ, and Lumbers ER. The expression and localization of the human placental prorenin/renin-angiotensin system throughout

pregnancy: roles in trophoblast invasion and angiogenesis? *Placenta* 32: 956-962, 2011.
Ray SB, and Wadhwa S. Mu opioid receptors in developing human spinal cord. *J Anat* 195 (Pt 1): 11-18, 1999.
Sarnat HB, Nochlin D, and Born DE. Neuronal nuclear antigen (NeuN): a marker of neuronal maturation in early human fetal nervous system. *Brain Dev* 20: 88-94, 1998.
Scain AL, Le Corronc H, Allain AE, Muller E, Rigo JM, Meyrand P, Branchereau P, and Legendre P. Glycine release from radial cells modulates the spontaneous activity and its propagation during early spinal cord development. *J Neurosci* 30: 390-403, 2010.
Slater R, Cantarella A, Gallella S, Worley A, Boyd S, Meek J, and Fitzgerald M. Cortical pain responses in human infants. *J Neurosci* 26: 3662-3666, 2006.
Slater R, Fabrizi L, Worley A, Meek J, Boyd S, and Fitzgerald M. Premature infants display increased noxious-evoked neuronal activity in the brain compared to healthy age-matched term-born infants. *Neuroimage* 52: 583-589, 2010a.
Slater R, Worley A, Fabrizi L, Roberts S, Meek J, Boyd S, and Fitzgerald M. Evoked potentials generated by noxious stimulation in the human infant brain. *Eur J Pain* 14: 321-326, 2010b.
Snider WD, Zhang L, Yusoof S, Gorukanti N, and Tsering C. Interactions between dorsal root axons and their target motor neurons in developing mammalian spinal cord. *J Neurosci* 12: 3494-3508, 1992.
Tadros MA, Farrell KE, Schofield PR, Brichta AM, Graham BA, Fuglevand AJ, and Callister RJ. Intrinsic and synaptic homeostatic plasticity in motoneurons from mice with glycine receptor mutations. *J Neurophysiol* 111: 1487-1498, 2014.
Tadros MA, Harris BM, Anderson WB, Brichta AM, Graham BA, and Callister RJ. Are all spinal segments equal: intrinsic membrane properties of superficial dorsal horn neurons in the developing and mature mouse spinal cord. *J Physiol* 590: 2409-2425, 2012.
Vermeren M, Maro GS, Bron R, McGonnell IM, Charnay P, Topilko P, and Cohen J. Integrity of developing spinal motor columns is regulated by neural crest derivatives at motor exit points. *Neuron* 37: 403-415, 2003.
Vinay L, Brocard F, and Clarac F. Differential maturation of motoneurons innervating ankle flexor and extensor muscles in the neonatal rat. *Eur J Neurosci* 12: 4562-4566, 2000a.
Vinay L, Brocard F, Pflieger JF, Simeoni-Alias J, and Clarac F. Perinatal development of lumbar motoneurons and their inputs in the rat. *Brain Res Bull* 53: 635-647, 2000b.
Walker SM, Franck LS, Fitzgerald M, Myles J, Stocks J, and Marlow N. Long-term impact of neonatal intensive care and surgery on somatosensory perception in children born extremely preterm. *Pain* 141: 79-87, 2009.
Walsh MA, Graham BA, Brichta AM, and Callister RJ. Evidence for a critical period in the development of excitability and potassium currents in mouse lumbar superficial dorsal horn neurons. *J Neurophysiol* 101: 1800-1812, 2009.
Weidenheim KM, Epshteyn I, Rashbaum WK, and Lyman WD. Neuroanatomical localization of myelin basic protein in the late first and early second trimester human foetal spinal cord and brainstem. *J Neurocytol* 22: 507-516, 1993.
Woodbury CJ, and Koerber HR. Widespread projections from myelinated nociceptors throughout the substantia gelatinosa provide novel insights into neonatal hypersensitivity. *J Neurosci* 23: 601-610, 2003.

Ye JH, Zhang J, Xiao C, and Kong JQ. Patch-clamp studies in the CNS illustrate a simple new method for obtaining viable neurons in rat brain slices: glycerol replacement of NaCl protects CNS neurons. *J Neurosci Methods* 158: 251-259, 2006.
Yoshimura M, and Jessell TM. Membrane properties of rat substantia gelatinosa neurons in vitro. *J Neurophysiol* 62: 109-118, 1989.
Ziskind-Conhaim L. Electrical properties of motoneurons in the spinal cord of rat embryos. *Dev Biol* 128: 21-29, 1988.
Zouikr I, Tadros MA, Barouei J, Beagley KW, Clifton VL, Callister RJ, and Hodgson DM. Altered nociceptive, endocrine, and dorsal horn neuron responses in rats following a neonatal immune challenge. *Psychoneuroendocrinology* 41: 1-12, 2014.

738 ***Figure Legends***

739

740 ***Figure One. Location of recorded neurons***

741 **A**. Image of a transverse spinal cord slice (300 μm thick) at 10 WG held in place by
742 nylon netting (vertical lines). **B**. Images of representative DH (left panel) and VH
743 (right panel) neurons at 16 WG. Note the clear difference in neuron soma size for
744 neurons at microelectrode tip. It was difficult to obtain recordings in DH neurons
745 younger than 16 WG (see text for details). **C**. Schematic representation of the location
746 of each recorded neuron. Recordings were made in DH (open circles) and VH (filled
747 circles) neurons across all age groups examined.

748

749 ***Figure Two. Action potential discharge patterns in fetal spinal neurons***

750 **A**. Neurons responded to depolarizing square current step injection (20 or 50 pA
751 increments, 800 or 1000 ms duration, inset lower right) in one of four ways: *tonic*
752 *firing* neurons discharged APs for the entire duration of the injected current; *initial*
753 *bursting* neurons discharged a burst of APs at the onset of the current step; *single*
754 *spiking* neurons discharged a single AP at the onset of each current step; and *reluctant*
755 *firing* neurons did not discharge APs in response to square current step injection.
756 Representative traces are from VH neurons aged 16-18 WG in response to 100 and
757 200 pA current steps, dashed line indicates -60 mV. **B**. The incidence of each of the
758 responses displayed in A for DH neurons aged 16-18 WG. No AP discharge was
759 observed in DH neurons prior to 16 WG (see text). **C.** The incidence of each response
760 profile displayed in A for VH neurons at each age group. Tonic firing was the most
761 commonly observed discharge pattern and its incidence increased with age. The
762 prevalence of reluctant firing neurons decreased with age.

763

764

765 ***Figure Three. Responses to hyperpolarizing current in dorsal and ventral horn***
766 ***neurons***

767 **A.** Neurons responded to hyperpolarizing square current step injection (-20 or -50 pA
768 increments, 800 or 1000 ms duration, inset lower right) in one of four ways: *passive*
769 responses were characterized by a lack of any active conductances during or after
770 hyperpolarization; *rebound spiking* was evident with AP discharge upon release from
771 hyperpolarization; *sag* was observed as a slow depolarization occurring during the

hyperpolarizing step; and a few neurons exhibited a sag during the hyperpolarizing step plus an *extended hyperpolarization* at the end of the current step. Representative traces are from VH neurons aged 16-18 WG, with the defining characteristic for each category indicated by a filled arrowhead. **B**. The incidence of each response in A, for DH neurons aged 16-18 WG. Prior to 16 WG, DH neurons displayed the passive response (see text). **C**. The incidence of each response in A, for VH neurons of each age group. Rebound spiking decreased and the other response types emerged with increasing age.

Figure Four. Intrinsic and AP properties of dorsal and ventral horn neurons

A. Bar plots for intrinsic properties of dorsal (DH, n = 9) and ventral (VH, n = 22) neurons capable of AP discharge. Input resistance (left) was lower in VH neurons, ($p = 0.05$). Rheobase current (centre) was trending towards larger values in VH neurons, however this was not significant ($p = 0.29$). Resting membrane potential (RMP, right) was similar in DH and VH neurons. **B**. Representative trains of AP discharge (left) from spontaneously active dorsal (top) and ventral (bottom) neurons. Dashed line indicates -70 mV. Single APs from each spinal cord location are expanded on the right, arrowheads denote AP threshold. **C**. Bar plots for AP properties measured on DH (n = 9) and VH (n = 22) neurons capable of AP discharge. AP threshold (top left) did not differ between the two spinal cord locations. AP amplitude (top right) was greater in VH neurons ($p =0.015$). AP half-with (bottom left) was unchanged between DH and VH neurons. After-hyperpolarization (AHP) amplitude (bottom right) was greater in VH neurons ($p = 0.001$). The number of cells in each age group denoted on each bar.

Figure Five. Changes in the properties of tonic firing ventral horn (VH) neurons during development

A. Bar plots displaying developmental changes in intrinsic properties of tonic firing VH neurons. Input resistance (left) decreased, rheobase (centre) increased, and resting membrane potential (right) was similar across the age groups examined. **B**. Some action potential properties differed during the developmental period examined. AP threshold (far left) was unchanged, whereas AP amplitude (centre left) increased from 10-12 WG to 16-18 WG. AP half-width decreased and AHP amplitude increased from 10 to 18 WG. * indicates $p < 0.05$, 10 – 12 WG vs 13-15 WG and 16-18 WG and #

806 indicates $p < 0.05$, 10-12 WG vs. 16-18 WG. The number of cells in each age group is
807 denoted on each bar.

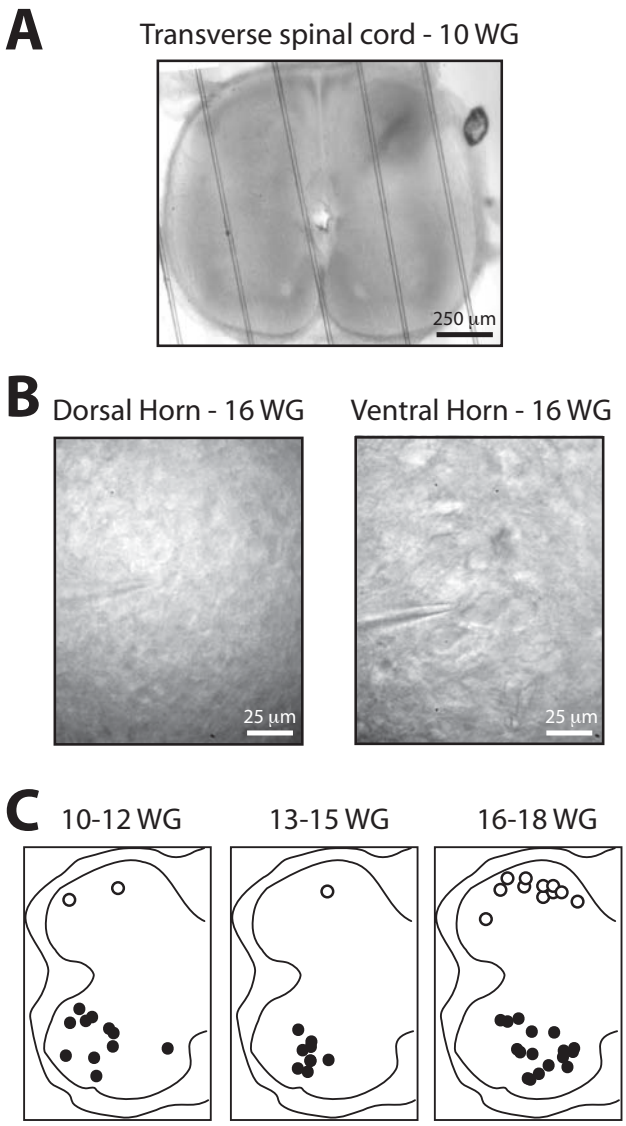

Figure 1
Tadros et al

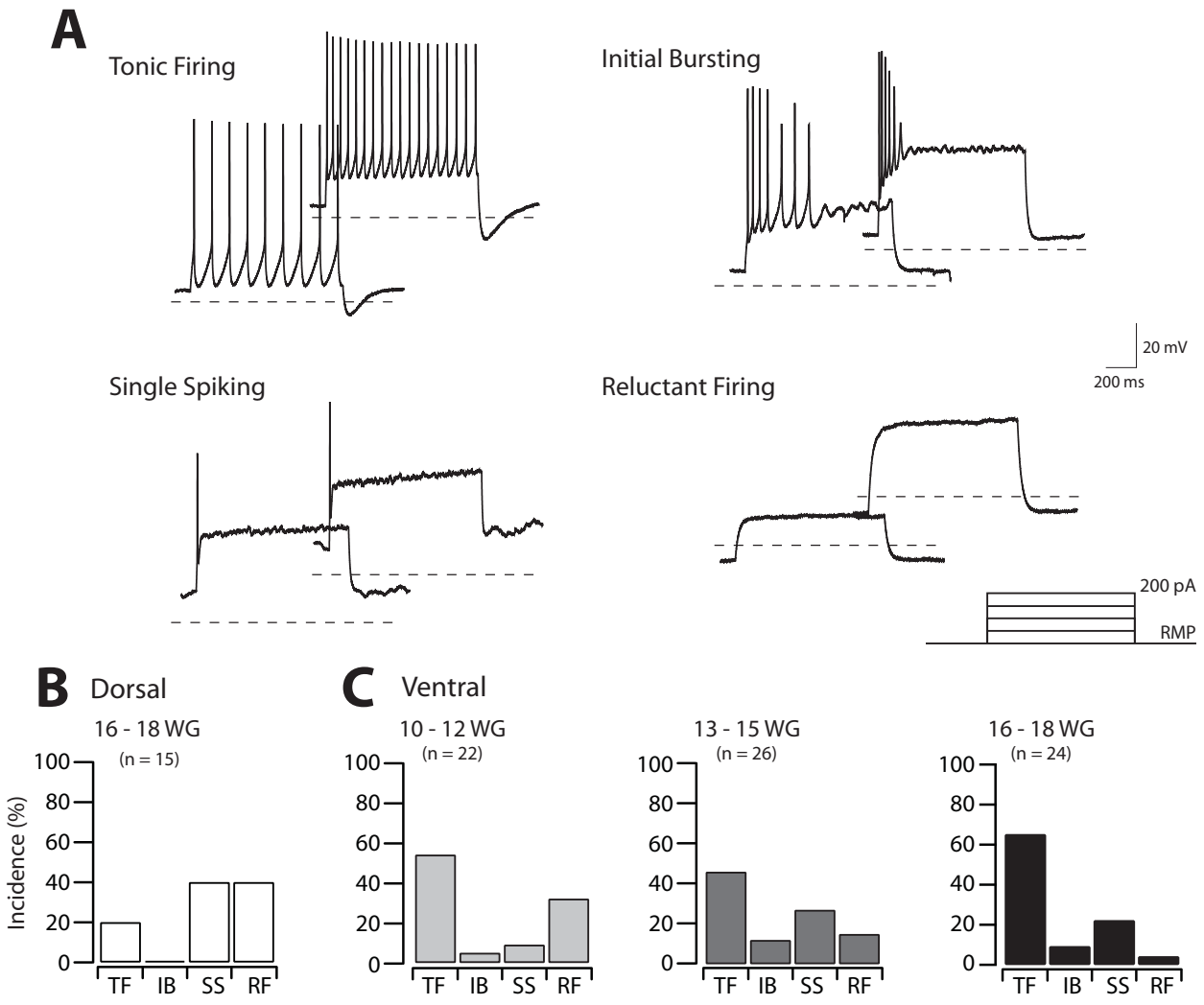

Figure 2
Tadros et al

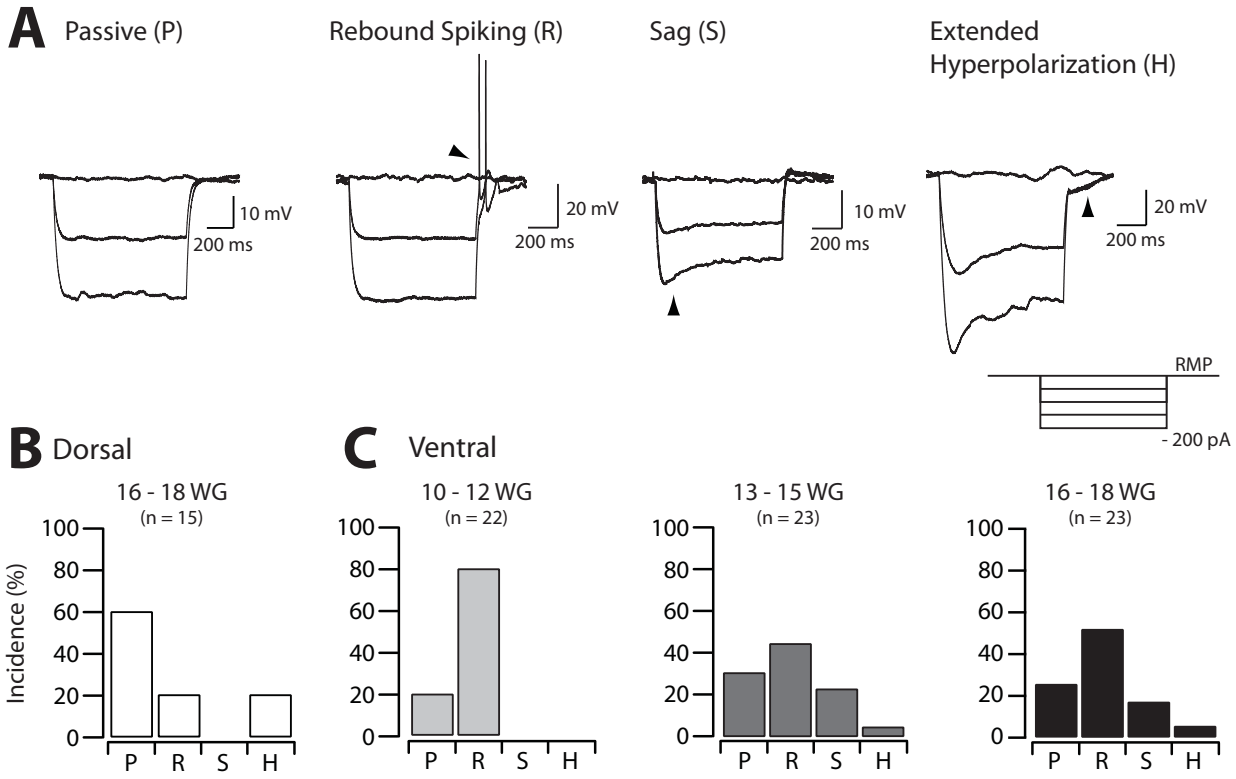

Figure 3
Tadros et al

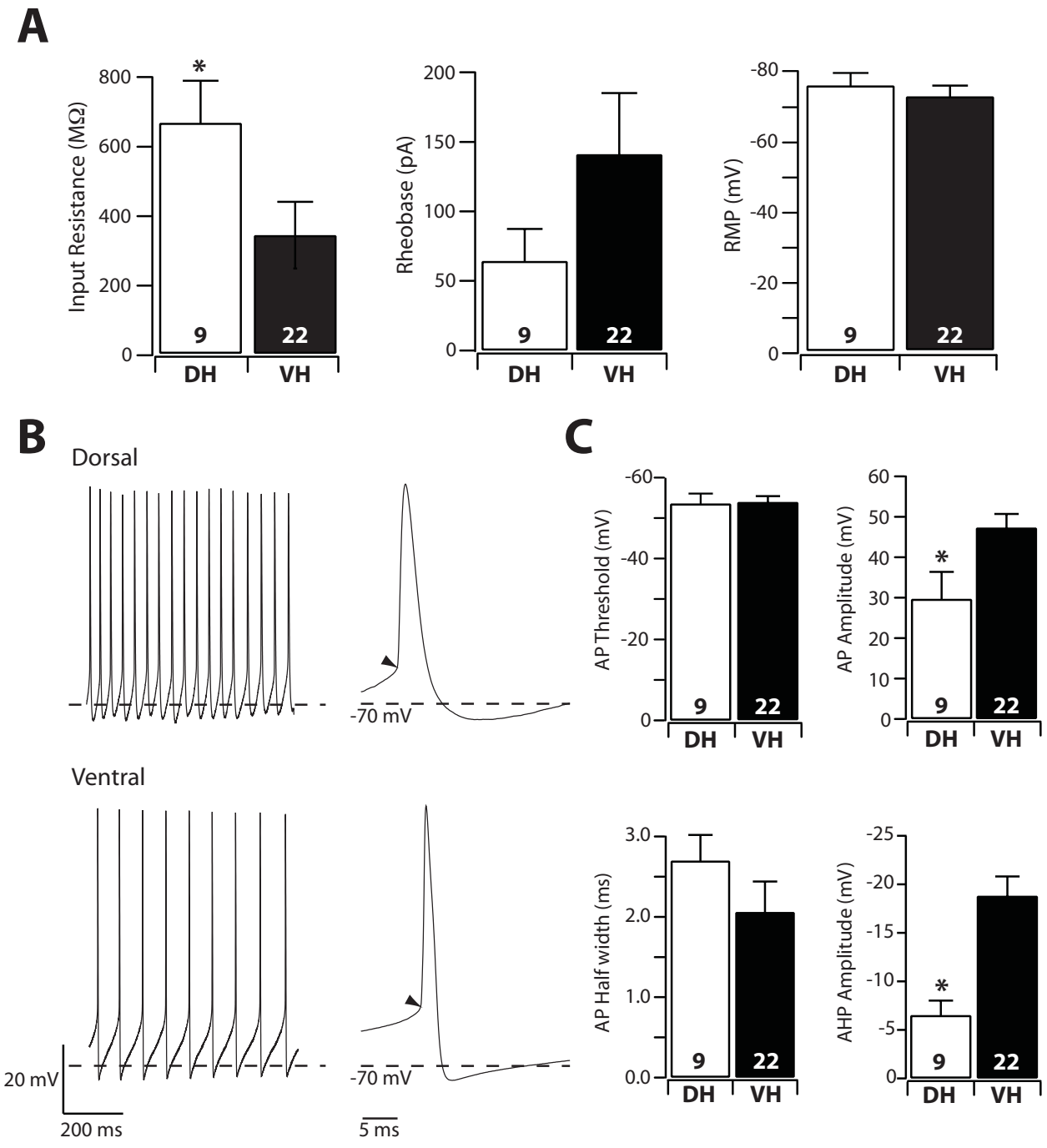

Figure 4
Tadros et al

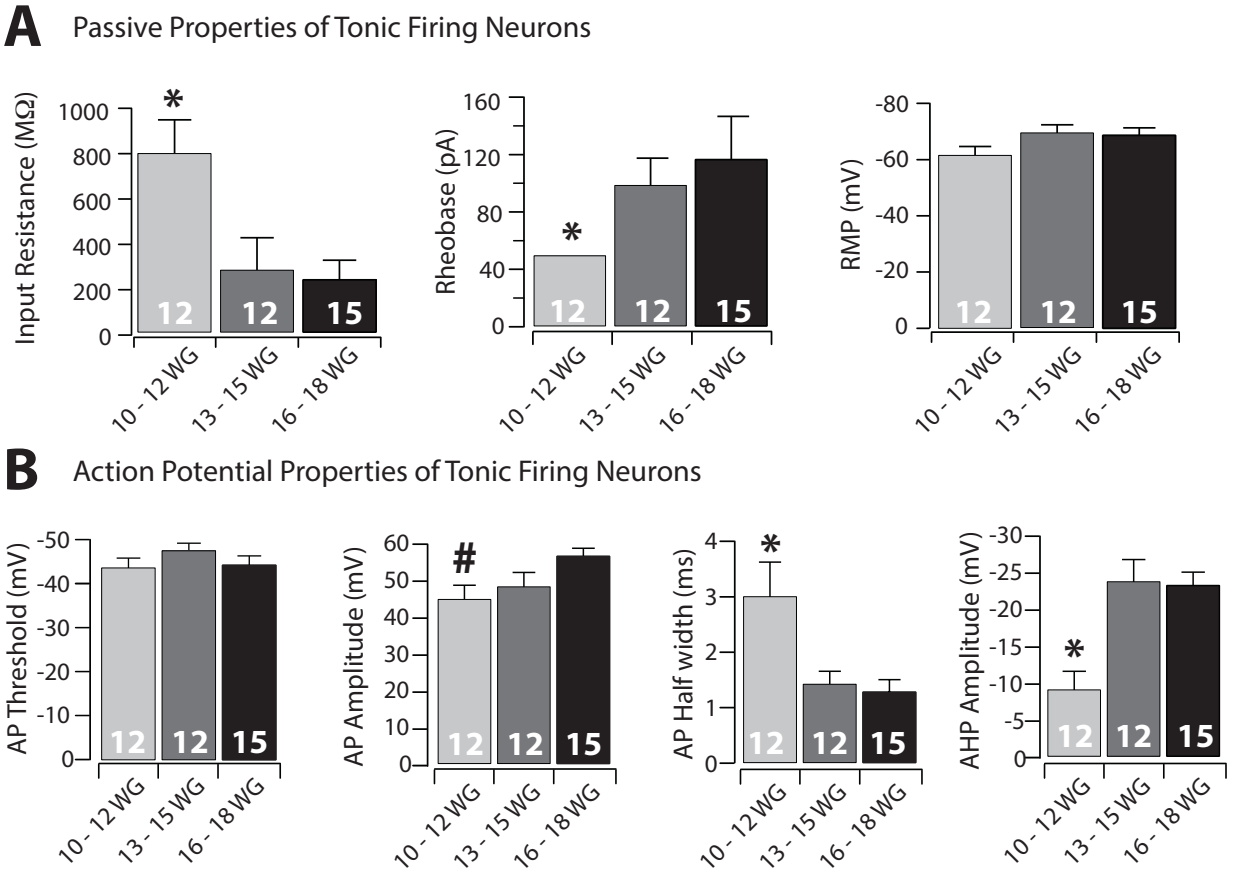

Figure 5
Tadros et al

Discharge Category	Region	Age	n	Input Resistance (MΩ)	RMP (mV)	Rheobase current (pA)	AP threshold (mV)	AP amplitude (mV)	AP half-width (ms)	AHP amplitude (mV)
Tonic Firing	Dorsal	10-12 WG	0							
		13-15 WG	0							
		16-18 WG	3	533 ± 234	-67.3 ± 8.6	20 ± 0	-52.1 ± 3.2 †	46.0 ± 16.7	2.7 ± 0.7	-9.2 ± 2.0
	Ventral	10-12 WG	12	795 ± 145	-62.1 ± 2.9 †ζ	50 ± 0	-45.0 ± 1.3	44.8 ± 3.6	3.0 ± 0.6	-9.2 ± 2.4
		13-15 WG	12	279 ± 140	-70.5 ± 2.6 †ζ	99 ± 19 #	-48.1 ± 1.6 †	48.2 ± 3.7 †	1.44 ± 0.2 †	-23.8 ± 2.9 †
		16-18 WG	15	238 ± 83	-69.1 ± 2.4 #†	117 ± 30	-45.5 ± 1.3	56.5 ± 1.8 #†	1.3 ± 0.2 #	-23.3 ± 1.7 #†
Initial Bursting	Dorsal	10-12 WG	0							
		13-15 WG	0							
		16-18 WG	0							
	Ventral	10-12 WG	1	849	-85.6	100	-41.7	52.9	1.4	-16.7
		13-15 WG	3	429 ± 88	-60.8 ± 7.4	48 ± 2.5	-52.6 ± 3.0 †	53.5 ± 10.3 †	2.1 ± 0.7	-12.6 ± 3.1
		16-18 WG	2	332 ± 195	-51.0 ± 2.7	50 ± 0	-36.2 ± 4.4	35.8 ± 11.0	3.9 ± 0.2	-6.6 ± 6.4
Single Spiking	Dorsal	10-12 WG	0							
		13-15 WG	0							
		16-18 WG	6	730 ± 148	-65.9 ± 4.1	87 ± 31	-39.3 ± 1.5	21.5 ± 3.4	2.7 ± 0.4	-5.1 ± 1.8
	Ventral	10-12 WG	2	1488 ± 377	-44.5 ± 3.8	50 ± 0	-39.7 ± 3.9	37.0 ± 12.2	4.0 ± 2.4	-4.0 ± 7.7
		13-15 WG	6	450 ± 240	-51.0 ± 3.1	90 ± 21	-41.9 ± 2.1	27.8 ± 4.2	2.9 ± 0.4	-10.8 ± 3.6
		16-18 WG	5	653 ± 323	-52.4 ± 6.1	100 ± 27	-43.8 ± 2.6	24.2 ± 3.4	3.7 ± 1.2	-10.1 ± 3.0
Reluctant Firing	Dorsal	10-12 WG	2	2928 ± 1080	-33.1 ± 4.1					
		13-15 WG	1	873 ± 115	-56.1 ± 2.9					
		16-18 WG	6	1470 ± 363	-64.6 ± 7.8					
	Ventral	10-12 WG	7	836 ± 228	-45.0 ± 2.4					
		13-15 WG	4	861 ± 285	-40.9 ± 3.6					
		16-18 WG	1	322	-91.4					

Table 1. Intrinsic and AP properties for each of the observed discharge categories. All data presented at mean ± SEM. Significance between discharge categories within age groups denoted as follows: # denotes significantly different to initial bursting; † denotes significantly different to single spiking; ζ denotes significantly different to reluctant firing.